Volume 9, Issue 5, pp. 88-92, 2025.
International Journal of Scientific Engineering and Science
ISSN (Online): 2456-7361

Establishment of Material Removal Model in Magnetic Polishing Process with Minimum Maxim Combining 3D Nanocomposite Material (MoS2/Fe3O4)@rGO+SiC

Le Dang Ha[1], Tran Ba Anh[1,*]
[1]Hanoi University of Industry, 298 Cau Dien, Bac Tu Liem District, Ha Noi, Vietnam

***Abstract*— *In this study, a material removal model for surface finishing (MR) using a small polishing head with a permanent magnet is proposed. The small ball tip magnetorheological (MR) polishing process using a permanent magnet is applied in the machining of products with complex contour impurities with small defects or convex surfaces with small curvature radii. In this process, the magnitude of the magnetic field of the ball tip and the cutting application of the MR material act on the perfect surface, creating a shadow effect. This study presents and simulates the research and experiment of the polishing tool design process combining the grinding solution (MoS2/Fe3O4)@rGO+SiC to create polishing action. In this study, a 3D nanocomposite (MoS2/Fe3O4)@rGO with the ability to absorb the magnetic field generated by the moving magnetic polishing head significantly was synthesized through the hydrothermal method and chemical cabinet finishing. The fusion of Fe3O4 from the calculation with rGO and MoS2 helps to optimize the parameters. In addition, to improve the polishing performance for this process, Silicon Carbide material. Process design and implementation simulations were performed to evaluate the surface finish and material removal performance. Simulation results and experimental data showed that high surface roughness was achieved without damaging or affecting the surface. The underlying mechanism of the material removal process was also studied and discussed.*

***Keywords*— *MRF (Material Removal Finishing), MR.*

I. INTRODUCTION

The new surface finishing process (Material Removal - MR) using small polishing heads in the form of permanent magnets belongs to the group of magnetic grinding and polishing (Magnetic Finishing – MRF)[1]. These methods exploit magnetic fields to control the abrasive grain or force applied to the artistic surface. Unlike the work using grinding wheels in polishing, it is not possible to achieve details with complex contours or with radius of curvature. Small ball tip magnetorheological polishing with permanent magnets is a specialized polishing method[2, 3]. This head consists of a hemispherical permanent magnet 4 mm in diameter and 5 mm in length, connected by a stainless steel rod. This design allows for the processing of miniature results with complex three-dimensional surfaces. something that is difficult to achieve with traditional machining methods . We know that the importance of surface quality in machined components is becoming increasingly essential[4].

In addition, the polishing solution used in this process also plays an extremely important role. In this study, the nanocomposite material we used is (MoS2/Fe3O4)@rGO combined with SiC abrasive material. In this study, nanocomposites (MoS2/Fe3O4)@rGO with multifunctional structures were designed and synthesized based on their components and microstructures[5]. Their magnetic absorption performance and absorption mechanism were studied to provide documentation for this process. A brief analysis of the above nanocomposite materials shows that: MoS2 is a layered (2D) semiconductor material with good electromagnetic and magnetic properties[6]. Fe_3O_4 (Magnetite) is a strong magnetic material (ferromagnetic), which can be controlled by a magnetic polishing head to enhance control of the machining process. In addition, rGO is a material that increases durability as well as dispersion and surface area. Next high hardness quality SiC master ball material is applied in target polishing ball[7].

Next, a 3-flat tool is adopted in our study of polishing from this feature. This machine consists of three linear motion axes, a main shaft, a slot shaft and a polishing wheel shaft[8]. The column and the polishing wheel are not in a three-axis linkage structure. The X and Y axes are arranged in a superposition to support the screw shaft and the illusion of performing horizontal movement[9]. The Z pad is applied to control the top gloss. The angle between the polishing wheel and the horizontal glass is 45 degrees, which helps to minimize the minimum when polishing unevenly shaped parts.

This directly affects the interaction of the material with the environment as well as its durability and mechanical properties. Upgrading the surface quality brings many benefits such as reduced friction, increased service life and most importantly improved product performance. This process uses the interaction between the magnetic tip fields and the magnetic abrasive grain to create a micro-ablation behavior on the machined surface, effectively removing the excess area . The efficiency of the MRF process depends on the rheological response of the ball fluid when in continuous contact with the field of the ball magnet . Static and process simulations throughout the entire process are fully implemented to analyze special materials and base surface finishes.

International Journal of Scientific Engineering and Science
Volume 9, Issue 5, pp. 88-92, 2025. ISSN (Online): 2456-7361

II. Process for creating MoS2, MoS2/Fe3O4 and (MoS2/Fe3O4)@RGO.

The steps for the preparation of MoS2 by the one-step hydrothermal method are illustrated in Figure 1(a). The steps for the preparation of flower-like MoS2/Fe3O4 powder and (MoS2/Fe3O4)@RGO powder are shown in Figures 1(b) and (c)[10].

Four standardized powder electromagnetic parameters were measured by coaxial method. The minimum total reflection was calculated based on the transmission line reason. Black (MoS2/Fe3O4)@RGO powder was mixed with paraffin in a mass ratio of 4:6 and pressed into a ring under 2.5 Mpa pressure.

This concentric ring has an inner diameter of 3 mm, an outer diameter of 7.0 mm, and a scan height of 3 mm. The detailed fabrication processes of MoS2, MoS2/Fe3O4, and (MoS2/Fe3O4)@RGO are provided in the supplementary material[11].

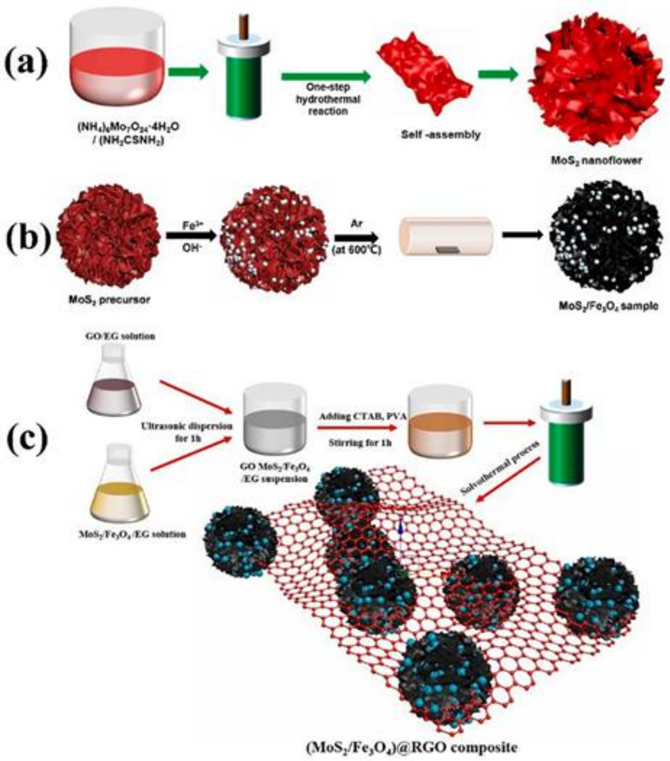

Figure 1. Process of making MoS2, MoS2/Fe3O4 and (MoS2/Fe3O4)@RGO.

III. Magnetic polishing method using ball tool.

To finish the precision parts with complex complexities, a polishing head made of NdFeB permanent magnet material was used in the simulation process. The polishing head, with a diameter of 4 mm, was precisely manufactured and mounted on a screw tool to ensure the shape accuracy such as concentricity and tight connection without breaking during machining [12]. In the magnetic fields generated by the polishing head, the magnetorheological fluid forms a flexible polishing layer with high slow speed that adheres evenly to the surface of the polishing head and is controlled by the high-speed rotation of the polishing head. This creates a dynamic flow of the MR solution at the polishing distance, which helps to apply dynamic application and cutting application to the test surface to achieve material removal during the polishing process. Figure 2 is a schematic diagram of the MRF polishing head process[13].

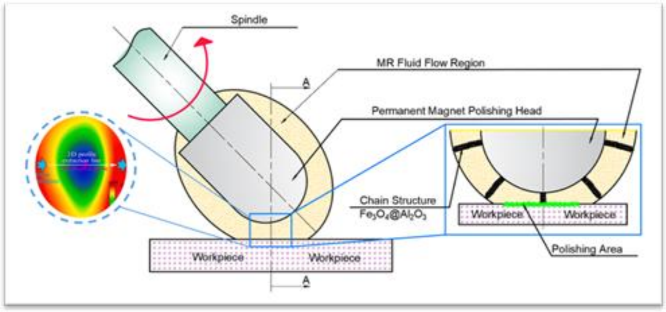

Figure 2 : Schematic diagram of the publishing mechanism for the first polishing part.

The polishing mechanism, process and material removal method in this study are solved as follows. When the polishing head is being safeguarded, the magnetorheological (MR) waste is uniformly attracted to the entire area of the polishing head due to the magnetic force of the permanent magnet. Its displacement retardation increases abruptly, causing it to change from the wild state to the semi - solid state [14]. When the cutting response is larger than the running response, the MR waste changes from the semi- solid state to the velocity state. When the magnetorheological waste changes, the abrasive particles impact on the surface at the fastest speed under the action of the application and the cutting application, causing the micro- material removal action. Theoretical calculations indicate that the polishing hole is located directly below the ball head [15]. In this study, we propose to create a new method to establish the image MRR by using the limit element simulation.

IV. Magnetic field analysis of permanent magnet polishing head, impact zone and material removal ability.

In order to generate and collect relatively accurate simulation data for future practical experiments. The simulation software we used is COMSOL Multiphysicals. In the finite element simulation, we used a 1:1 scale model of the designed polishing ball head and it is clearly illustrated in Figure 3. The origin of the technical system is located at the center of the active area on the surface of the material. Illustration of the polishing on the surface in OXY basis . Its size is 5 × 5 × 1.5 mm and the magnetorheological (MR) emitter covers the surface evenly with a thickness of 1.5 mm . The size of the air regions around the polishing area is set to 20 × 20 × 20 mm and the angle between the crankshaft of the magnet ball head and the machined surface is 45 °. The simulation parameters are the parameters that will be used for future calculation[16]: the gap between the polishing head and the surface is 0.5 mm and the rotational speed of the ball head is simulated at 5,000 rpm.

International Journal of Scientific Engineering and Science
Volume 9, Issue 5, pp. 88-92, 2025.
ISSN (Online): 2456-7361

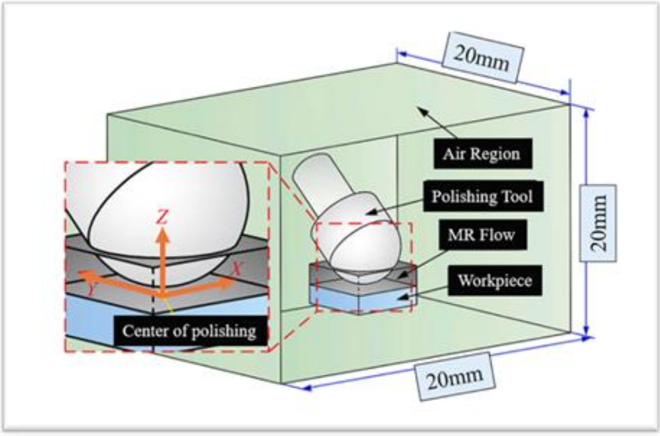

Figure 3 : Schematic diagram of finite element simulation model and engineering system .

4.1. Magnetic Analysis Of Permanent Male Polishing Head .

The magnetic field analysis of the polishing head gives us the results illustrated in Figure 4. The static magnetic module is used in COMSOL Multiphysical Analysis to analyze the magnetic field around the polishing head. Since the polishing head is a symmetrical mass rotating around its axis, we simulate and analyze it in a simplified way by analyzing on a cross-section passing through its axis. The element ownership limit of the ball is set to magnetize vertically and downwards towards the tool surface.

The redundant password is used to model the strong response from the ball head, as shown in method (1)[17].

$$B = \mu_o \mu_{rec} H + B_r \qquad (1)$$

where μ_0 is the vacuum confirmation magnetization (H/m), μ_rec is the confirmation magnetization , H is the magnetic field strength (A/m) and B_r is the residual magnetic flux density (T).

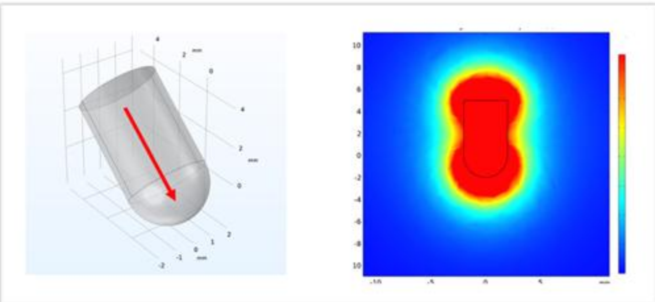

Figure 4: Description of the polishing tool

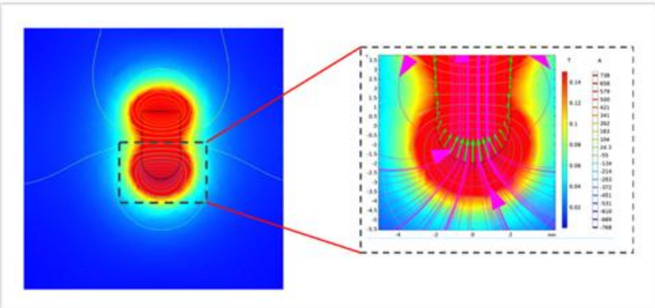

Figure 5: Simulation, analysis of large urban areas and magnetic field lines.

Through simulation we get the determined density fields which are uniformly distributed throughout the polishing set and more especially at the beginning and end of the maxim. Furthermore, a stronger magnetic field significantly affects the material removal properties of this technique. From figure 5 we get the larger speed from the largest information currently used in this process and the progress is at 0.14-0.2T. Since the magnet polishing top creates a magnetic field around it, the polishing solution carries magnetic properties that align, direct the magnetic field parameters and return.

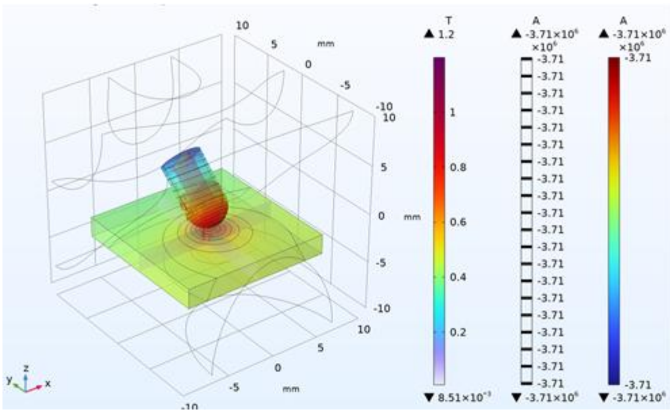

Figure 6 : 3D simulation image of the magnetic field generated by the maxim .

4.2. Divide The Areas of the Active Shadow Onto The Beauty Surface.

Before applying the analysis to the polishing zone, it is necessary to determine its boundaries. The polishing zone is defined by the contact points between the polishing tool and the surface, which create shapes similar to those of the polishing tool. Based on the magnetic analysis presented in the previous section, you can find that the polishing zone is elliptical. However, during the polishing process, the polishing fluid is compressed, resulting in deviations from the perfect ellipse.

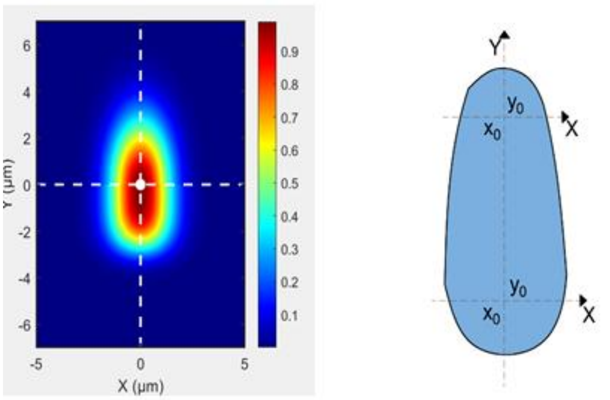

Figure 7: Polishing lines on the surface.

Assuming the oranges in the compressed image follow a two-dimensional Gaussian normal distribution, the general model is given by:

International Journal of Scientific Engineering and Science
Volume 9, Issue 5, pp. 88-92, 2025. ISSN (Online): 2456-7361

$$f(x,y) = A\exp\left(-\frac{(x-x_0)^2}{2\sigma_x^2} - \frac{(y-y_0)^2}{2\sigma_y^2}\right) \quad (3)$$

In there :

- A is the highest value of the distribution (corresponding to the red region on the color scale).
- (x_0, y_0) is the center of the region.
- σ_x and σ_y times as the width distribution in the x and y directions.

Total integral of the two-dimensional Gaussian distribution.
The integral of the function f(x, y) over the entire space is:

$$I = \int_{-\infty}^{+\infty}\int_{-\infty}^{+\infty} A\exp\left(-\frac{(x-x_0)^2}{2\sigma_x^2} - \frac{(y-y_0)^2}{2\sigma_y^2}\right)dxdy \quad (4)$$

Implement the properties of Gaussian analysis:

$$\int_{-\infty}^{+\infty} \exp\left(-\frac{x^2}{2\sigma_x^2}\right)dx = \sqrt{2\pi}\sigma_x \quad (5)$$

Similarly, for y, we have:

$$I = A.(\sqrt{2\pi}\sigma_x).(\sqrt{2\pi}\sigma_y)$$
$$I = A.2\pi\sigma_x\sigma_y \quad (6)$$

Typically, the orange zone falls within certain ranges, with limits such as:

$$\alpha A \leq f(x,y) \leq A$$

To analyze these ranges, we need to calculate:

$$I^{'} = \int_{vungmaucam} A\exp\left(-\frac{(x-x_0)^2}{2\sigma_x^2} - \frac{(y-y_0)^2}{2\sigma_y^2}\right)dxdy \quad (7)$$

4.3. Material Removal Capability and Action .

In this study, a simulation model based on the interaction between the polishing ball, the magnetic fluid and the workpiece surface is proposed to generate the cutting application. The cutting process application in the polishing process includes chemical and mechanical applications. According to Preston's material removal theory in glass polishing, the detailed MRR model is convenient for the application and the relative speed between the workpiece and the polishing plate.

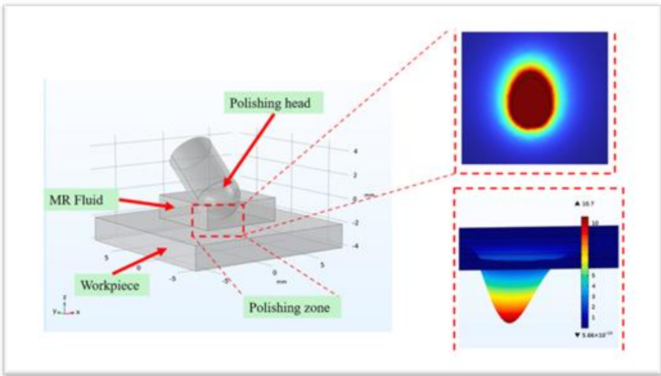

Figure 8: 3D simulation polishing.

We consider the material extracted from the variations under the influence of school activities as a Bingham material, which can be described by the method[17]:

$$\tau = \begin{cases} \eta_0 V + sign(v)\tau_0, |\tau| > \tau_0 \\ 0, |\tau| < \tau_0 \end{cases} \quad (8)$$

In which : τ is the cutting application of Bingham material, is τ_0 the application that depends on the magnetic field strength, η_0 is the initial speed and V is the cutting speed.
The cutting application is approximately symmetrical about the center line and distributed according to a Gaussian curve, in which the cutting application reaches its maximum value at the position closest to the machined surface and zero equilibrium at the end of the shadow combat zone.

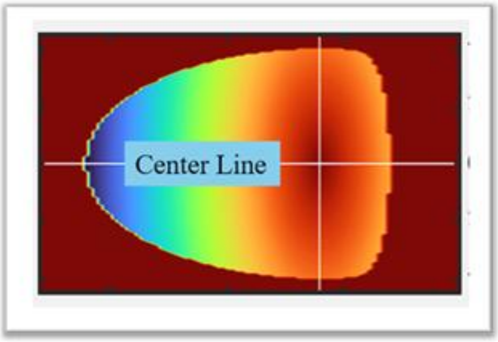

Figure 9: Performance analysis during polishing.

According to theoretical analysis, the material removal behavior in the polishing process using the first polishing command also depends on the largest division in the cutting application. Therefore, the Preston method is improved based on the cutting application and set up for the material removal simulation model as follows:

$$MRR = K\tau V \quad (9)$$

In which: *MRR* is the material type ability, K is the Preston coefficient including the effects of material parameters affecting the interaction between the machined part and the polishing, τ is the application of high speed cutting from the magnetic field and the polishing service creates the surface on the technological equipment. *V* is a speed ball war.

Magnetochemical application is an application related to the effect of magnetic fields on magnetic materials or substances, which can change the intrinsic performance, cutting application or rheological properties of the system. In ball Magnetic, it plays an important role in the work of Controlling the material removal process. The applied magnetization is calculated as follows[18]:

$$p_m = 3\omega\mu_0\mu_r(\mu_q - \mu_r)H^2 / 2(\mu_q + 2\mu_r) \quad (10)$$

where is ω the analyzable fraction of particles in the rheological release agent (MR), μ_0 is the vacuum resolution (H/m), μ_r is the manganese release agent resolution (H/m),

Volume 9, Issue 5, pp. 88-92, 2025. *ISSN (Online): 2456-7361*

μ_q is the confirmed level of magnetic particles (H/m) and H is the magnetic field strength (A/m).

V. CONCLUSION

Through the simulation process here, we have obtained the following results: Establishing the material removal mechanism in the polishing process using a magnetic ball head as a 40 degree tilt angle between the polishing head and the machined surface.

model by permanent magnet polishing abrasive grain finish found significant potential in improving surface quality, even for difficult-to-machine materials such as sapphire and titanium. However, there are still many limitations in this process such as the control of the head ball during the process with increasing border complexity. In the future, we will study to improve the process with more parameter settings such as the tilt angle between the polishing axis and the machined surface, the adjustment of the rotation speed as well as additional settings on the properties of the magnetic fluid.

In upcoming studies, we intend to use the suggested model for the surface finishing of other hard-to-machine materials, such as titanium alloys, SUS 304 stainless steel, K9 optical glass, YAG crystals, and various other challenging substances. This will allow us to assess the cost-effectiveness and practical outcomes of the model in a manufacturing setting to address these machining challenges.

REFERENCES

[1] Yang, Y., et al. A Magnetic Abrasive Finishing Process with an Auxiliary Magnetic Machining Tool for the Internal Surface Finishing of a Thick-Walled Tube. Machines, 2022. 10, DOI: 10.3390/machines10070529.

[2] 2Duy Trinh, N., et al., Application of magnetic liquid slurries and fuzzy grey analysis in polishing nickel-phosphorus coated SKD11 steel. Particulate Science and Technology, 2022. 40(4): p. 401-414.

[3] Liu, Z., et al., Modeling and simulation of workpiece surface flatness in magnetorheological plane finishing processes. The International Journal of Advanced Manufacturing Technology, 2020. 111: p. 1-15.

[4] Pan, J., et al., Research on material removal model and processing parameters of cluster magnetorheological finishing with dynamic magnetic fields. The International Journal of Advanced Manufacturing Technology, 2019. 100(9): p. 2283-2297.

[5] Wang, Z. and Q. Zhao, 3D flower-like (MoS2/Fe3O4)@rGO nanocomposites with remarkable EMW absorption property. Materials Letters, 2023. 337: p. 133993.

[6] Kalia, S., et al., Two-dimensional layered rGO-MoS2 heterostructures decorated with Fe3O4 nanoparticles as an electrochemical sensor for detection of para-nitrophenol. Journal of Physics and Chemistry of Solids, 2024. 184: p. 111719.

[7] Zhou, J., et al., Core-shell structured nanocomposites formed by silicon coated carbon nanotubes with anti-oxidation and electromagnetic wave absorption. Journal of Colloid and Interface Science, 2022. 607: p. 881-889.

[8] Wang, T., et al., Development of a Magnetorheological Finishing Machine for Small-Bore Part of Irregular Shape and Experimental Study. American Journal of Engineering and Applied Sciences, 2015. 8: p. 399-404.

[9] Arrasmith, S., et al., Use of magnetorheological finishing (MRF) to relieve residual stress and subsurface damage on lapped semiconductor silicon wafers. Proceedings of SPIE - The International Society for Optical Engineering, 2001. 4451.

[10] Guo, H., et al., State of the art recent advances and perspectives in 2D MXene-based microwave absorbing materials: A review. Nano Research, 2023. 16: p. 10287-10325.

[11] Fu, Z., et al., Research progress of ceramic matrix composites for high temperature stealth technology based on multi-scale collaborative design. Journal of Materials Research and Technology, 2022. 18: p. 2770-2783.

[12] Chen, M., et al., Model of the material removal function and an experimental study on a magnetorheological finishing process using a small ball-end permanent-magnet polishing head. Applied Optics, 2017. 56(19): p. 5573-5582.

[13] Liu, H., et al., Magnetorheological finishing of an irregular-shaped small-bore complex component using a small ball-end permanent-magnet polishing head. Nanotechnology and Precision Engineering, 2019. 2(3): p. 125-129.

[14] Salzman, S., et al., Magnetorheological finishing of chemical-vapor deposited zinc sulfide via chemically and mechanically modified fluids. Applied Optics, 2016. 55(6): p. 1481-1489.

[15] Alam, Z., F. Iqbal, and S. Jha, Automated control of three axis CNC ball end magneto-rheological finishing machine using PLC. International Journal of Automation and Control, 2015. 9: p. 201-210.

[16] Vijaya, A., Improvement in forming process using Magnetorheological Fluid Assisted Cushion in Hydraulic Press. IOP Conference Series: Materials Science and Engineering, 2020. 912: p. 032003.

[17] Tian, J., et al., A novel specialized material removal rate model considering the synergistic effect of dynamic pressure and shear stress for the permanent-magnet small ball-end magnetorheological polishing. Journal of Manufacturing Processes, 2023. 101: p. 1431-1442.

[18] Chen, C., et al. Research on the Magnetorheological Finishing Technology of a High-Steepness Optical Element Based on the Virtual-Axis and Spiral Scanning Path. Micromachines, 2024. 15, DOI: 10.3390/mi15091154.